

Fig. 5. Resistive-layer deposition patterns. The pattern on the right has overlaps; the pattern at left has none.

be achieved by depositing half the pattern elements on one side of the film and the other half on the other side.

V. CONCLUSIONS

The fact that capacitive impedance sheets can reduce the overall thickness and improve the bandwidth of Jaumann absorbers is not new, nor are the single-frequency notch design requirements, namely that Γ and its derivatives vanish at the single notch. What we have illustrated here is a double-notch design approach in which Γ is forced to zero at two frequencies instead of one. Unlike the single-notch design requirement, which generates a pair of equations whose solution is analytically tractable, at least for two or three sheets, the double-notch design requirement generates four second-degree equations in four unknowns, the solution of which is more troublesome. We relied here on a numerical minimization scheme to solve that system of equations.

The solution confirmed our hunch that the bandwidth of the double-notch design increases as the notch frequencies are spread further from the center frequency. The notches cannot be spread too far apart, however, lest the central peak rise above the -20 dB performance floor we arbitrarily imposed at the outset. The maximum notch displacement can be no more than 41% for this particular performance level.

Thus, if we take the trouble to attempt to find a solution, even if it demands the use of brute-force numerical methods, we find that we can expand the bandwidth considerably over that available from the single-notch design approach. We showed that a capacitive two-sheet double-notch Jaumann absorber can have a 20-dB bandwidth of 108% if the sheet spacing is fixed at $0.1875\lambda_0$ at the center frequency. And although laboratory tests of one design did not have the deep notches exhibited by our numerical design, its bandwidth was also about 108%.

The optimum two-sheet double-notch design therefore has more than four times the bandwidth of the classic Salisbury screen, but is only 1.5 times as thick. And although the double-notch design is more complicated, it can probably be implemented with very little effort using circuit-analog design tools and equipment.

REFERENCES

- [1] W. W. Salisbury, "Absorbent body for electromagnetic waves," June 10, 1954, US Patent no. 2,599,944.
- [2] W. H. Emerson, "Electromagnetic wave absorbers and anechoic chambers through the years," *IEEE Trans. Antennas Propagat.*, vol. AP-21, pp. 484-490, July 1973.
- [3] E. F. Knott, J. F. Shaeffer, and M. T. Tuley, *Radar Cross Section*, 2nd ed. Boston, MA: Artech, 1993, pp. 322-323.
- [4] L. J. du Toit, "The design of Jaumann absorbers," *IEEE Antennas Propagat. Mag.*, vol. 36, no. 4, pp. 17-25, Dec. 1994.
- [5] B. Chambers, "Frequency tuning characteristics of capacitively loaded Salisbury screen radar absorber," *Electron. Lett.*, vol. 30, no. 19, pp. 1626-1628, Sep. 15, 1994.

- [6] R. L. Fante and M. T. McCormack, "Reflection properties of the Salisbury screen," *IEEE Trans. Antennas Propagat.*, vol. 36, pp. 1443-1454, Oct. 1988.
- [7] L. J. du Toit, "Analysis and synthesis algorithms for the electric screen Jaumann electromagnetic absorber," Ph.D. dissertation, Univ. of Stellenbosch, Stellenbosch, South Africa, 1993.
- [8] W. H. Press, S. A. Teukolsky, W. T. Vetterling, and B. P. Flannery, *Numerical Recipes in FORTRAN*, 2nd ed. New York: Cambridge University Press, 1992, sec. 10.4.
- [9] E. F. Knott, "Radar observables," in *Tactical Missile Aerodynamics: General Topics*, M. Hensch, Ed. Washington, DC: AIAA (American Institute of Aeronautics and Astronautics), 1992, vol. 141, ch. 4, pp. 149-152.

Efficient Numerical Computation of Singular Integrals with Applications to Electromagnetics

Smain Amari and Jens Bornemann

Abstract—Efficient schemes to accurately compute singular integrals are presented. The singularity is removed prior to numerical integration, using a change of variables, integration by parts, or a combination of both. A change of variables eliminates power-law singularities of the type $x^{-\alpha}$, $\alpha < 1$ and renders the integrand well behaved. Similarly, a logarithmic singularity of the form $\ln x$ is eliminated either by direct integration by parts or by multiplying and dividing the integrand by $\ln x$ followed by integration by parts. Cauchy-type singularities are also removed by integrating the singular term by parts twice. In all cases, the remaining integrand is well behaved and lends itself to straightforward numerical integration. The technique is applied to scattering from a perfectly conducting cylinder. Comparison of the numerical and exact solutions show the stability of the technique.

I. INTRODUCTION

Many phenomena in engineering and physics are described by integral equations whose kernel often involves singularities of varied degrees. Integral formulations in electromagnetic problems, through Green's functions, require evaluation of singular integrals. The method of moments is a typical method which involves evaluation of singular integrals, especially the self-terms [1], [2]. Singh and Singh used the tanh map to transform a singular integral over a finite interval $[a, b]$ into a rapidly decreasing improper integral extending from $-\infty$ to $+\infty$ [3].

A popular method of evaluating singular integrals numerically consists of isolating the singularity while using the Gauss quadrature method [4]. In this method, the integration is taken from $a + \delta$ to b instead of from a to b where a and b are the limits of integration, and the integrand is singular at the point a . Increasingly smaller values of δ are taken until an acceptable accuracy is achieved. A second approach consists in subtracting, from the original integrand, a singular function whose antiderivative is known and which approaches the integrand in the neighborhood of the singularity [5]. A drawback of this method is the fact that it involves subtraction of numbers which can be extremely large, for the function is singular, and may lead to erroneous results if higher accuracy is required.

Manuscript received February 2, 1995; revised April 14, 1995.

The authors are with the Laboratory for Lightwave Electronics, Microwaves, and Communications (LLiMiC), University of Victoria, Victoria BC, V8W 3P6, Canada.

IEEE Log Number 9414671.

Power-law singularities can be integrated through a change of variables whereby the singularity is eliminated [6]. Also, open formulas tailored to a host of singularities can be derived [6]. The singularity is, however, still present in this last approach.

In this paper, we present simple techniques which are applicable to a variety of singularities encountered in modeling of electromagnetic fields. The approach presented here always first removes the singularity and then carries out numerical integration on the remaining well-behaved integrand. Logarithmic singularities are handled using integration by parts until the singularity is removed. Integration by parts is also efficient in accurately evaluating singularities of the Cauchy type.

Two-dimensional scattering problems in electromagnetics involve Hankel functions which are singular at the origin. To test the numerical stability of the algorithms presented here, the induced current density on a perfectly conducting cylinder is calculated through the method of moments and compared to the analytical solution. We show that the numerical solution converges to the exact current distribution as the number of basis functions is increased.

II. POWER-LAW SINGULARITIES

In this section we show how power-law singularities of the form $x^{-\alpha}$, $\alpha < 1$ can be treated. The case $\alpha = 1$, which roughly corresponds to Cauchy singularities where the integral is interpreted in the sense of its principal part, is treated separately.

Consider the following integral

$$I_1 = \int_a^b f(x) dx. \quad (1)$$

The function $f(x)$ is assumed singular at the point $x = a$ where it can be approximated by $Cx^{-\alpha}$ where C is a constant and α a parameter which determines the "order" of the singularity. The case where the function is singular at both end-points can be treated by dividing the interval $[a, b]$ into two subintervals and treating each one of them separately. There is, therefore, no loss of generality in our assumption. We also take a to be zero and $b = 1$; this can always be done using a linear transformation. The change of variables

$$t = x^{1-\alpha} \quad (2)$$

allows us to rewrite the integral I_1 as [6]

$$I_1 = \frac{1}{1-\alpha} \int_0^1 f[t^{(1/1-\alpha)}] t^{(\alpha/1-\alpha)} dt. \quad (3)$$

It can be seen easily that the singularity is now eliminated from the integrand; standard Gauss quadratures can be used to accurately and efficiently evaluate it if $f(x)$ is any given function exhibiting a power-law singularity. As a typical example, consider the case where $f(x) = 1/\sqrt{x}$. Using (3) with $\alpha = 1/2$, the exact result follows straightforwardly

$$I_1 = \int_0^1 \frac{dx}{\sqrt{x}} = \frac{1}{\frac{1}{2}} \int_0^1 \frac{1}{\sqrt{t^2}} t dt = 2. \quad (4)$$

The same transformation can also be used to evaluate singular integrals whose behavior at one end-point is the product of a natural logarithm and a term $x^{-\alpha}$. This is the case of $\ln(x)/\sqrt{x}$, for example. Since the singularity in $1/\sqrt{x}$ is stronger than the logarithm, the change of variable used above also eliminates the singularity. In this

specific example, the integrand is transformed to

$$\int_0^1 \frac{\ln(x)}{\sqrt{x}} dx = 2 \int_0^1 t \ln(t) dt \quad (5)$$

which is again well behaved and can be straightforwardly integrated. The case of isolated logarithmic singularities, i.e., where the function behaves as $\ln(x)$, $x \rightarrow 0^+$ cannot be treated by this change of variables. It is discussed in the next section.

III. LOGARITHMIC SINGULARITIES

Consider a singular integral where the integrand has a logarithmic singularity at $x = 0$

$$I_2 = \int_0^1 f(x) dx, \quad f(x) \sim \ln x, \quad x \rightarrow 0^+. \quad (6)$$

Because of the singularity, direct numerical integration, especially for those methods using end-points, will certainly fail. It is very important in all cases of singular integrals to first attempt to eliminate the singularity since it is assumed to be integrable. For this particular case, an integration by parts along with an appropriate splitting of the original interval of integration lead to a well-behaved integrand. Since the singularity is present only at $x = 0$, we concentrate on the interval $[0, 0.5]$. The threshold 0.5 was chosen so it would not hit the zero of the logarithm; this becomes clear shortly. We rewrite the corresponding contribution to (6) in the following form

$$I_2' = \int_0^{0.5} \left[\frac{f(x)}{\ln(x)} \right] \ln(x) dx. \quad (7)$$

Note that the quantity in brackets is well behaved at $x = 0$, the singularity having been incorporated in the last logarithm term. It is now also evident why the point $x = 1$ has been avoided. A simple integration by parts leads to

$$I_2' = [x \ln(x) - x] \frac{f(x)}{\ln(x)} \Big|_0^{0.5} - \int_0^{0.5} (x \ln x - x) \left[\frac{f(x)}{\ln(x)} \right]' dx. \quad (8)$$

Again, the singularity has been removed, since the integrand in (8) is finite at $x = 0$. If (8) is applied to the function $f(x) = \ln x$, the second term vanishes, leading to the exact result without any need for numerical integration. It is this feature of analytically including as much of the *a priori* knowledge we have about the integrand that makes the present approach powerful.

It is also possible to eliminate the logarithmic singularity by direct integration by parts. If the integrand in (6) is written as the product of unity (1) and $f(x)$, then integration by parts leads to

$$I_2 = xf(x) \Big|_0^1 - \int_0^1 xf(x)' dx. \quad (9)$$

Since the function $f(x)$ approaches $\ln(x)$ as x approaches zero, both terms in (9) are well defined.

A different type of singularity that is often encountered is the Cauchy principal value integral which in rough terms corresponds to $\alpha = 1$ in (3). Obviously the change of variables utilized above fails [see (3)]. Again integration by parts can be fruitfully used in this situation.

IV. CAUCHY-TYPE SINGULARITIES

In a Cauchy-type singularity, the integral is interpreted as a principal part. There are a number of techniques to evaluate this type of singular integrals with varied degrees of accuracies. Gauss

quadratures are often used along with the trick of subtraction of singularity [5]. It is also possible to set up quadratures, by a proper choice of mesh points and weights, which are exact for polynomials of a given order [5]. An alternative approach consists in expanding the function in a Taylor series around the singularity [$x = y$ in (10) below]. The following discussion assumes that the function $f(x)$ is a known smooth function in the sense that its first and second derivatives are finite in the interval $[a, b]$. The important case where the function is known only numerically, either from previous numerical computation or measurement, can be handled adequately using substitutional formulas [7], [8]; this case is not covered here.

Consider the integral

$$I_3(y) = P \int_a^b \frac{f(x)}{x-y} dx. \quad (10)$$

Here, P denotes the Cauchy principal value. The function $f(x)$ is assumed well behaved such that the integral exist for values of y in the interval $[a, b]$. Following the present approach, we first try to eliminate the singularity and only then carry out the numerical integration. An integration by parts leads to

$$I_3(y) = \ln|x-y| f(x) \Big|_a^b - \int_a^b \ln|x-y| f(x)' dx. \quad (11)$$

If the derivative $f(x)'$ vanishes at $x = y$, the integrand in this equation is no longer singular, and numerical integration can be used at this stage. If this is not the case, then a second integration by parts is necessary to eliminate the singularity. The second derivative of $f(x)$ is now needed, but the elimination of the singularity far outweighs the effort that goes into evaluating the second derivative. For such a situation, the integral is rewritten as

$$I_3(y) = \ln|x-y| f(x) \Big|_a^b - [(x-y) \ln(x-y) - (x-y)] f(x)' \Big|_a^b + \int_a^b [(x-y) \ln|x-y| - (x-y)] f(x)'' dx. \quad (12)$$

Unless generated by the second derivative, the singularity at $x = y$ is now eliminated since the integrand is well behaved. If the present approach is applied to a polynomial, (12) always leads to stable numerics. It is even possible to render the integrand in the remaining integral in (12) smoother by subtracting the quantity $f(y)''$ (the second derivative of $f(x)$ evaluated at $x = y$) from the integrand such that both terms in the integrand vanish as x approaches y .

Another singularity which is often encountered in electromagnetics, especially in planar circuits, is the Maxwellian singularity $1/\sqrt{1-x^2}$. This case is simply handled through the change of variables

$$x = \sin(\theta). \quad (13)$$

The remaining integrand is again well behaved and poses no significant stability problems. Note also that this last singularity can be efficiently dealt with using Gauss-Chebyshev quadratures whose weight function is $1/\sqrt{1-x^2}$ [6].

V. NUMERICAL RESULTS

The approach presented here is first applied to an integral which has both a power-law and a logarithmic singularity. This is the example discussed in [3], namely the evaluation of the following integral

$$I_1 = \int_0^1 \frac{\ln x}{\sqrt{x}} dx. \quad (14)$$

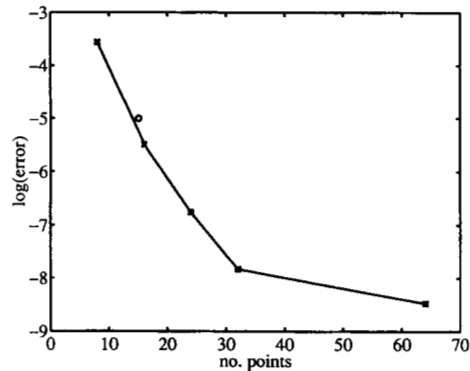


Fig. 1. Error in evaluating the integral I_2 (16) for different numbers of integration points. The circle is from [3], the crosses from the present work.

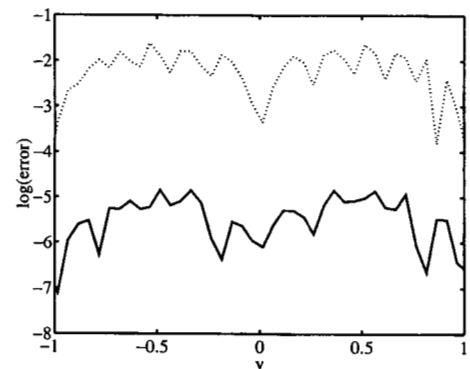


Fig. 2. Error in the principal part of $f(x) = x^4 - 1, |x| \leq 1$ for 16 (dotted line) and 96 (solid line) integration points.

Applying the change of variables discussed above, we rewrite this integral as

$$I_1 = 4 \int_0^1 \ln x dx. \quad (15)$$

Equation (15) has a logarithmic singularity which is removable by integrating by parts. This leads to the exact answer $I_1 = -4$. This simple example shows that an attempt to remove the singularity led directly to the exact answer. Obviously in more complex situations the singularity will be removed, but the exact answer is not expected. As a second example, we compute the integral I_2 in [3] using the change of variables in (13). I_2 is given by

$$I_2 = \int_0^1 \frac{T_2(x) \cos(10x)}{\sqrt{1-x^2}} dx = -\frac{\pi}{2} J_2(10). \quad (16)$$

Here $T_2(x)$ is the second-order Chebyshev polynomial, and $J_2(x)$ is the second-order Bessel function of the first kind. Fig. 1 shows the variation of the error as the number of integration points is changed. The circle is the minimum error from [3] for $N = 15$ and the crosses are from the present work for $N = 8, 16, 24, 32,$ and 64 . Clearly the elimination of the singularity not only stabilizes the computation but, in this case at least, converges rapidly to the exact answer. As a third example, the method used in eliminating the Cauchy-type singularity is applied to the function $f(x) = x^4 - 1, |x| \leq 1$. The corresponding integral can be calculated exactly and is given by

$$P \int_{-1}^1 \frac{x^4 - 1}{x - y} dx = 2y^3 + \frac{2}{3}y + (y^4 - 1) \ln \left| \frac{1-y}{1+y} \right|. \quad (17)$$

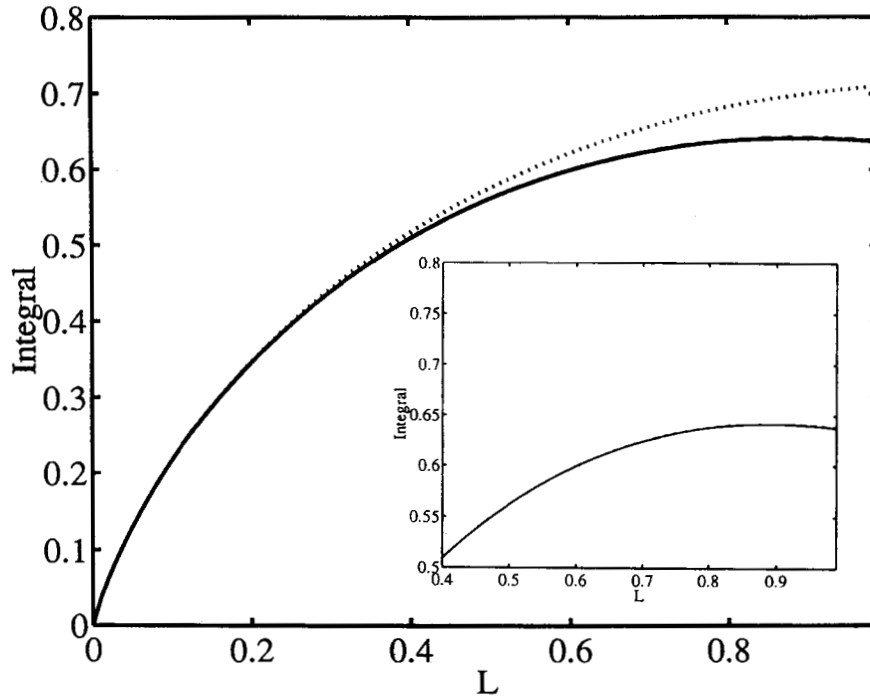


Fig. 3. Imaginary part of the integral in (19) as a function of L . The small-argument approximation [2] (dashed line) and the present work (solid line). Same integral using two points (inset dotted line) and 32 points (solid line) in the Gauss quadratures.

Fig. 2 shows the error for 16 and 96 integration points in Gauss quadratures through (12) as a function of y in the range $[-1, 1]$. The error consistently decreases as the number of integration points increases. Further increase did not affect the stability of the results as expected from the fact that the singularity has been removed. Note that the trick of subtracting the singularity along with Gauss quadratures gives the exact result when the function $f(x)$ is a polynomial, and enough points are used as long as the points falling close to the singularity are properly handled. Otherwise, the trick of subtracting the singularity amounts to computing the ratio

$$R = \frac{f(x) - f(y)}{x - y} \quad (18)$$

which is not stable in the limit $x \rightarrow y$ [9].

The final example is a singular integral which appears in the method-of-moments solution to two-dimensional electromagnetic problems, especially in the surface integral equation approach. Indeed the problem of scattering from a conducting cylinder involves self-terms which require the evaluation of the singular integral [2, pp. 184, 221]

$$S = \int_0^L H_0^{(2)}(k_0 x) dx. \quad (19)$$

Here $H_0^{(2)}(x)$ is the Hankel function of the second kind of order zero. For small values of L , more precisely of the product $k_0 L$, the small-argument approximation of the Hankel function is used to evaluate S leading to the following imaginary part [2, p. 185]

$$\Im[S] = -\frac{2}{\pi} L \left[\ln \left(\frac{\gamma k_0 L}{2} \right) - 1 \right] \quad (20)$$

where $\gamma = 1.781$ is Euler's constant ($\ln \gamma = 0.5772$).

The logarithmic singularity in the integrand in (19) can be removed using the methods presented here. For simplicity we set k_0 to unity

(1); this amounts to a simple scaling operation. Integration by parts gives

$$S = x H_0^{(2)}(x) \Big|_0^L - \int_0^L x H_0^{(2)}(x)' dx. \quad (21)$$

Using the identity $H_0^{(2)}(x)' = -H_1^{(2)}(x)$ and the fact that $x H_0^{(2)}(x)$ vanishes in the limit $x \rightarrow 0$, we get

$$S = L H_0^{(2)}(L) + \int_0^L x H_1^{(2)}(x) dx. \quad (22)$$

It can be seen easily that the remaining integrand is now well behaved since the term x cancels the singularity in the Hankel function of the second kind of order 1, $H_1^{(2)}(x)$.

Fig. 3 shows a plot of the imaginary part of S evaluated using the present approach (solid line) and the method used in [2] (dotted line). It can be seen clearly that the two techniques coincide for values of L smaller than about 0.4. For L larger than 0.4, the small-argument approximation in [2] fails and produces up to 11% higher values (at $L = 1$) than our numerical integration technique which is valid for all values of L . The inset in Fig. 3 illustrates the convergence and stability of the method based on removing the singularity before numerical integration. The dotted line depicts the imaginary part obtained from only two points in the Gauss quadrature and the solid line from 32 points. The difference between the two is minimal for $0 \leq L \leq 1$. In addition, the numerical stability of the technique based on the removal of the singularity allows us to test the accuracy of the small-argument approximation used in evaluating this type of singular integrals.

VI. APPLICATION TO SCATTERING FROM A CYLINDER

As an application of the schemes presented here, the induced current distribution on a perfectly conducting cylinder of ra-

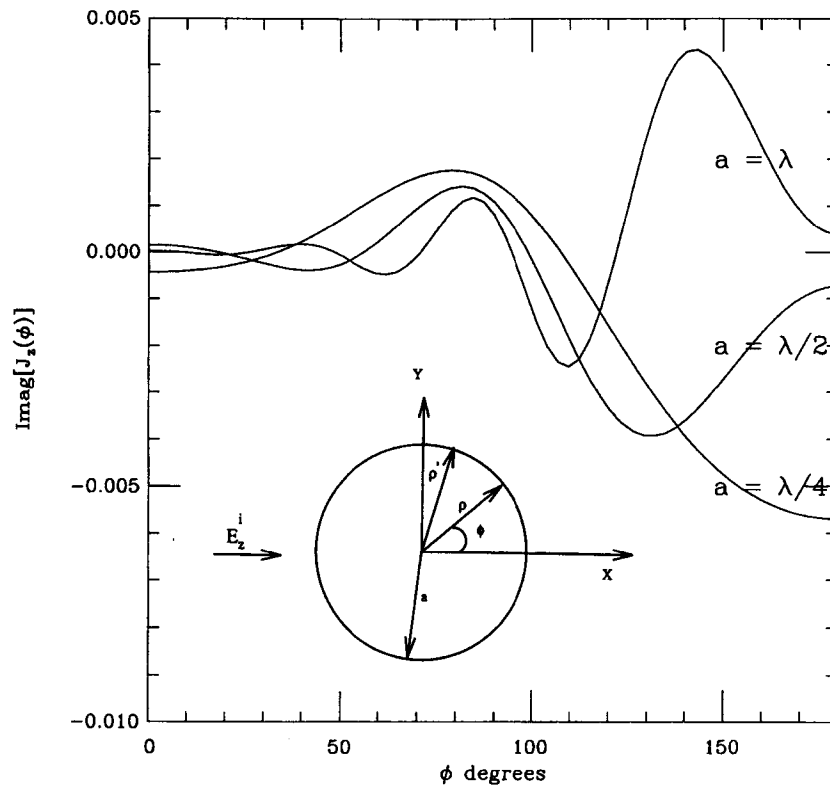
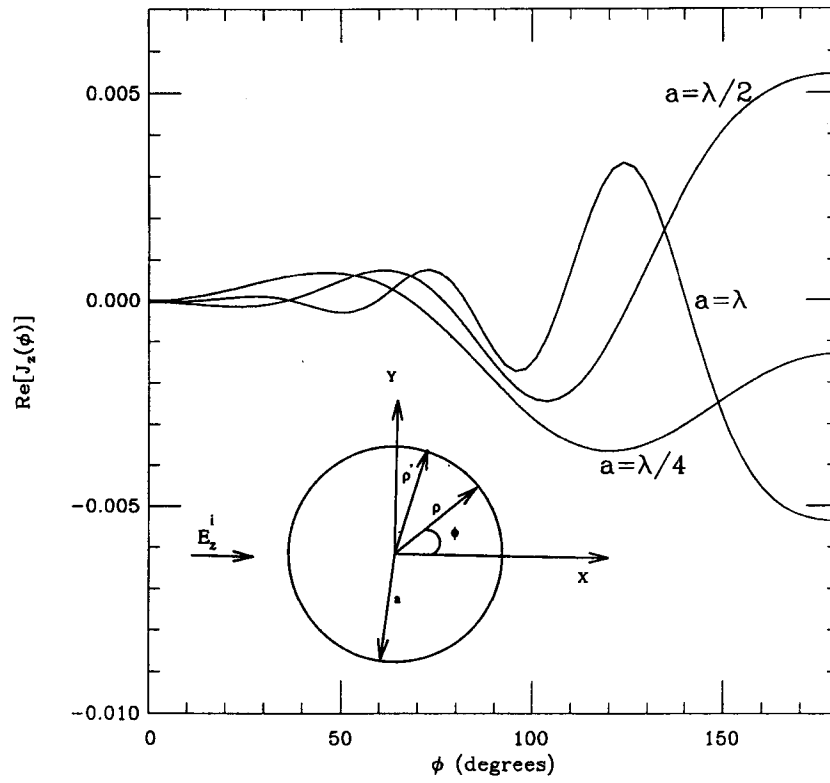


Fig. 4. Real and imaginary parts of the current density induced by an incident TM plane wave polarized along the axis of the cylinder for $a = \lambda/4$, $\lambda/2$, and λ : (a) real part and (b) imaginary part.

radius a is calculated through a method-of-moment solution. The cylinder is considered. The structure is shown in the inset in Fig. 4.

The induced current density on the cylinder is easily shown to satisfy the following integral equation [1, p. 42]

$$E_z^i(\rho) = \frac{k\eta}{4} \int_C J_z(\rho') H_0^{(2)}(k|\rho - \rho'|) dl', \quad \rho \in C \quad (23)$$

where E_z^i is the incident electric field and J_z the induced current density. If E_z^i is taken as a plane wave propagating along the x -axis, namely

$$E_z^i = e^{-jkx} \quad (24)$$

then an exact analytical solution is known and is given by [10, p. 233]

$$J_z(\phi) = -\frac{2}{\omega\pi\mu a} \sum_{n=-\infty}^{n=+\infty} \frac{j^{-n} e^{jn\phi}}{H_0^{(2)}(ka)}. \quad (25)$$

The circumference of the cylinder is now divided into N equal sectors centered at $\phi_n = [2\pi(n-1)/N]$. A pulse function is assumed on each sector. The method of moments solution to (23) is then reduced to a matrix equation relating the expansion coefficients of the current density to the incident electric field through an impedance matrix whose entries are

$$l_{mn} = \frac{k\eta}{4} \int_{C_n} H_0^{(2)} \left[k\sqrt{(x-x_m)^2 + (y-y_m)^2} \right] dl_n. \quad (26)$$

Using polar coordinates, l_{mn} can be rewritten as

$$l_{mn} = \frac{ka\eta}{4} \int_{\Delta\phi_n} H_0^{(2)} \left[2ka \sin \left(\frac{\phi - \phi_m}{2} \right) \right] d\phi_n. \quad (27)$$

The integrand in (27) has a logarithmic singularity as ϕ approaches ϕ_m . The techniques of Section III and (20)–(22) are now applied to compute l_{mn} .

It is convenient to rewrite the differential $d\phi_n$ as $d(\phi_n - \phi_m)$ since ϕ_m is constant. Integration by parts leads to

$$\begin{aligned} l_{mn} = & \frac{ka\eta}{4} \\ & \cdot \left\{ (\phi - \phi_m) H_0^{(2)} \left[2ka \sin \left(\frac{\phi - \phi_m}{2} \right) \right] \right\} \Big|_{\phi_n - \Delta\phi_n/2}^{\phi_n + \Delta\phi_n/2} \\ & + ka \int_{\phi_n - \Delta\phi_n/2}^{\phi_n + \Delta\phi_n/2} (\phi - \phi_m) H_1^{(2)} \\ & \cdot \left[2ka \sin \left(\frac{\phi - \phi_m}{2} \right) \right] \cos \left(\frac{\phi - \phi_m}{2} \right) d\phi. \end{aligned} \quad (28)$$

Note that both terms are now finite for all values of m and n . It is also not necessary to make the approximation of point source for $m \neq n$ since all of the integrals can be computed directly.

The numerical results obtained using (28) are presented in Fig. 4(a) and (b). Both the real and imaginary parts of the induced current density are plotted as a function of the angle ϕ for values of $a = \lambda/4, \lambda/2$, and λ . The analytical and numerical solutions are plotted simultaneously. The two solutions agree to within the fifth digit after the decimal point; they agree within plotting accuracy. Note that the wave is incident at $\phi = 180$ degrees and not $\phi = 0$. The numerical results were obtained using 128 basis functions. We intentionally used a large number of basis function to test the stability of the integration technique in the limit of small intervals. Larger numbers were also tested and gave stable and increasingly accurate solutions.

VII. CONCLUSIONS

An efficient scheme to compute singular integrals is presented. A combination of integration by parts and change of variables can be used to remove integrable singularities. The remaining integrands are well behaved and pose no serious numerical problems. Power-law singularities can be removed through a change of variables, whereas integration by parts eliminates logarithmic singularities. Two successive integrations by parts also eliminate the singularity from the Cauchy principal value integrals. Typical examples taken from the literature, some with known closed-form solutions, were used to illustrate the stability and the convergence of the approach. The technique was used to calculate the induced current density on a perfectly conducting cylinder. The stability of the numerical solution was verified by comparing the analytical and numerical solutions which agree well.

REFERENCES

- [1] R. F. Harrington, *Field Computation by the Moment Methods*. Malabar, FL: Krieger, 1987.
- [2] J. J. H. Wang, *Generalized Moment Methods in Electromagnetics*. New York: Wiley, 1991.
- [3] R. Singh and S. Singh, "Efficient evaluation of singular and infinite integrals using the tanh transformation," *IEE Proc. Microwave Antennas Propagat.*, vol. 141, no. 6, pp. 464–466, Dec. 1994.
- [4] W. Cheney and D. Kincaid, *Numerical Mathematics and Computing*. Monterey: Brooks, 1985.
- [5] P. J. Davis and P. Rabinowitz, *Methods of Numerical Integration*. Orlando, FL: Academic, 1984.
- [6] W. H. Press *et al.*, *Numerical Recipes*. New York: Cambridge Press, 1986, ch. 3.
- [7] S. Amari, "Evaluation of Cauchy principal-value integrals using modified Simpson rule," *Appl. Math. Lett.*, vol. 7, no. 3, 1994, pp. 19–23.
- [8] S. Amari, M. Gimersky, and J. Bornemann, "Imaginary part of antenna's admittance from its real part using Bode's integrals," *IEEE Trans. Antenna Propagat.*, vol. 43, pp. 220–223, Feb. 1995.
- [9] S. E. Koonin and D. C. Meredith, *Computational Physics*. New York: Addison Wesley, 1990, pp. 3–5.
- [10] R. F. Harrington, *Time-Harmonic Electromagnetic Fields*. New York: McGraw-Hill, 1961.

Comments on "Experimental and Theoretical Comparison of Some Algorithms for Beamforming in Single Receiver Adaptive Arrays"

Yimin Zhao and Dehang Ju

In the above paper,¹ B. G. Wahlberg, I. M. Y. Mareels, and I. Webster present a simple algorithm to estimate the covariance matrix by perturbing the weights \mathbf{W} .

Section II, however, contains two errors. The basic error is in (17). This leads to errors in (18).

Manuscript received January 4, 1995.

Y. Zhao is with the Department of Microwave Telecommunication Engineering, Xidian University, Xi'an, 710071, People's Republic of China.

D. Ju is with Xi'an Institute of Space Radio Technology, CAST, Xi'an, 710000, People's Republic of China.

IEEE Log Number 9414742.

¹B. G. Wahlberg, I. M. Y. Mareels, and I. Webster, *IEEE Trans. Antennas Propagat.*, vol. 39, no. 1, pp. 21–28, Jan. 1991.